CONTOUR-SHAPE BASED RECONSTRUCTION OF FRAGMENTED, 1600 B.C. WALL PAINTINGS

by

C. Papaodysseus[1*], Th. Panagopoulos[1], M. Exarhos[1], C. Triantafillou[1], D. Fragoulis[1], C. Doumas[2]

1. National Technical University of Athens,
Department of Electrical and Computer Engineering, Division of Computer Science,
9 Heroon Polytechneiou, GR-15773, Athens, GREECE.

2. National University of Athens, Akrotiri Excavations,
Thera, GREECE.

*Corresponding author, e-mail: cpapaod@cs.ntua.gr

EDICS Categories: 1-TREC, 6-PATT

Permission to publish this Abstract separately is granted.

ABSTRACT

In this paper a novel general methodology is introduced for the computer-aided reconstruction of the magnificent wall-paintings of the Greek island Thera (Santorini), painted in the middle of the second millennium BC. These wall-paintings are excavated in fragments and, as a result, their reconstruction is a painstaking and a time-consuming process. Therefore, in order to facilitate and speed up this process a proper system has been developed based on the introduced methodology. According to this methodology each fragment is photographed, its picture is introduced to the computer, its contour is obtained and subsequently all fragments contours are compared in a manner proposed herein. Both the system and the methodology presented here, extract the maximum possible information from the contour shape of fragments of an arbitrary initially unbroken plane object, to point out possible fragments matching. This methodology has been applied to two excavated fragmented wall-paintings consisting of 262 fragments, with full success but most important it has been used to reconstruct, for the first time, unpublished wall-paintings parts from a set of 936 fragments.

A. INTRODUCTION-PROBLEM DESCRIPTION

The discovery of the wall-paintings at Akrotiri of the Greek island Thera (Santorini), is of outstanding importance for human knowledge of the early Aegean world and not only. According to prominent archaeologists these wall-paintings rank alongside the greatest archaeological discoveries. The late professor Marinatos originated the excavations, which are now successfully continued by Professor Christos Doumas. As with the treasures of Pompeii and Herculaneum, the wall-paintings of Thera were preserved due to the seal of the pumice from the great eruption of a volcano [1]. As a rule, the walls decorated with paintings no longer survive. They collapsed together with their painted coat before the volcanic eruption, due to particularly strong earthquakes. Thus, a single painting is usually scattered into many fragments mixed with the fragments of other wall-paintings, too. The restoration of the wall-paintings from the fragments is a very painstaking and time consuming process frequently demanding many months or even years of dedicated, experienced personnel work for a single wall-painting restoration. Therefore, the development of a system that will contribute to the automatic restoration of these wall-paintings is of fundamental importance for this archaeological research, but for many others too, which face the problem of an image reconstruction from excavated fragments.

Each excavated wall-painting fragment after being cleaned, is being photographed with a very strict protocol, so that very similar illumination conditions, a fixed distance of the fragment plane from the camera focus and minimal photo distortion are ensured. Subsequently, the obtained image is processed and eventually each photographed fragment is embedded into a white background frame, which we call the absolute frame of reference of the specific fragment (see Figure 2).

The problem of automatic reconstruction of wall-paintings includes pattern classification. This is a field where extensive research has been done the last decades [2], [3], [4], [24]. Several object recognition systems use low level vision modules which operate upon images in order to derive depth measurements. Other systems employ bottom-up description of images to generate viewpoint-invariant groupings of image features [5] or they use generalized cylinders for the description of

model and scene objects [6], [7], [8]. When a very large number of objects is to be recognized hypothesis and tests methods are frequently employed [9], [10], [11], [12]. CAD-based object recognition is currently studied [3], [13], [14], [15], [16], while algorithms have been designed using topologically equivalent classes called aspect graphs [17], [18], [19], [20], [21], [22], [23]. Considerable research on object recognition using invariants has been done the last years [36], [37], [38], [39].

The problem tackled in this paper may be considered to be associated with automatic jigsaw puzzle solving, too. However, as we will point out below, the two problems solutions manifest drastic and essential differences. In fact, a number of papers deal with automatic puzzle solving: In [31] a set of critical points, the isthmus point and the isthmus critical points that define a feature used in matching partial boundaries is employed. A similar global feature of isthmus is used for automatic jigsaw puzzle solving in [32]. In [29] a global jigsaw puzzle assembly algorithm is used consisting of two major substeps. The frame of the puzzle is assembled first and it is used as a starting point for assembling the entire puzzle; the global assembly is made via a method analogous to the "traveling salesman problem". In [30] the individual sides of each puzzle piece are spotted first, the corners are detected next and eventually various features (side curvature, convexity/concavity, Euclidean distance between adjacent corners etc.) to be used in the matching of the puzzle pieces are obtained. Similarly, [28], [33], [34], [35] employ the method of extracting critical points from local border information.

The problem of automatic reconstruction of the prehistoric city of Thera wall-paintings is in essence drastically different than the one of automatic jigsaw puzzle solving. In fact,

1. No a priori knowledge concerning the shape of each piece (fragment) is given and therefore one cannot presuppose the existence of breakpoints on the boundary curve of it. Actually, in practice, many fragments boundary curves have no breakpoints. As a consequence, division of the piece boundary in sides is totally meaningless, as well as corner detection.
2. No frame pieces exist, i.e. pieces whose at least one side is a straight line segment. Hence, the strategy of starting the puzzle solution from the frame reconstruction is equally meaningless and the jigsaw puzzle solution cannot be considered equivalent to the traveling salesman problem.
3. The fragments size and shape varies dramatically in contrast to what happens in jigsaw puzzles.

4. Characteristic features such as side curvature, convexity/concavity, Euclidean distance between adjacent corners etc., cannot contribute to our problem solution since we expect, practically with certainty, that gaps exist between adjacent fragments of each wall-painting, due to wear.
5. No a priori knowledge about the picture content exists.
6. No unique solution concerning the matching of two fragments exists.
7. Due to the possible gaps between adjacent wall-painting fragments an alternative local curve matching procedure to the one described in [28], [29], [31], [34] etc., has been developed and is introduced in this paper.
8. Finally, very frequently, many different wall-paintings are excavated mixed altogether, due to the collapse of the two or three floor building whose walls were initially decorated by those paintings.

Hence, one may state that the problem of the automatic jigsaw puzzle solution is a "subcase" of the problem tackled in this paper. In fact, one may define the approach introduced here as an attempt to extract the maximum possible information from the contour of a set of fragments in order to achieve the initial image/object reconstruction. Therefore, the method introduced here and the related system can be very well employed to reconstruct any broken into fragments object employing contour shape information only.

Although the method and system presented here have proven very powerful in reconstructing wall paintings for the first time, we must stress that, if one wishes to develop a complete system of automatic reconstruction of an image from its constituent fragments, one may take into account many other parameters, too, such as a) matching between internal contours of the fragments b) colour continuation between actually adjacent fragments, c) continuation of the thematic content d) crack continuation e) geological texture of the side opposite to the painted one, etc.

B. PRELIMINARY FRAGMENTS PROCESSING

B.1 Obtaining the fragment image and its contour

Fragments are embedded very carefully into thin sand along with a colour palette and a scale so that proper processing can be applied later to compensate possible colour and size discrepancies

due to different shooting conditions (see Figure 1). The fragments digital images are stored in a database and processed for quality improvement. Subsequently, “fragment extraction” takes place, in the sense that specific developed image segmentation algorithms are applied to the obtained image in order to separate each fragment from the background. Thus, finally, one obtains each fragment embedded into a white background, at a random position. This fragment positioning together with axes is considered to be "the absolute reference system or frame" for each fragment separately, in all subsequent analysis (see Figure 2).

Next, each fragment contour is obtained using the following quite classical method:

- The colour depth of each fragment (piece) is decreased from millions of colours to black and white. So, the whole fragment is black (value “1”) and its background white (value “0”).
- The fragment contour is extracted. However, no edge detection algorithm could generate the fragment contour in the form necessary for the subsequent analysis. In fact, as it will become evident from the subsequent analysis, in order that the introduced methodology is applied, each contour must have the following properties: A) each pixel must have exactly two neighbouring pixels B) no isolated pixels or groups of pixels are allowed and C) three pixels must not form a compact right (90^o) angle.

Therefore, a software is developed to guarantee this form of the contour.

B.2 Obtaining rotated contours to cope with random fragment orientation

Consider two actually adjacent fragments. Since their orientation in their absolute frame of reference is completely random, it follows that in order to make them match one must perform a random rotation to at least one of them. In order to account for this random rotation, the contours of each fragment are built corresponding to all fragment orientations obtained after repeated rotation of $STEP$ degrees. To set ideas, if one chooses $STEP = 1^0$ then one must perform 360 rotations to the initially obtained contour around the origin of axes of the absolute frame of reference, thus obtaining 360 contours for each fragment. Notice, that, clearly, since each fragment can be considered as a rigid body, rotation around another centre is a composition of a parallel translation and rotation around the

axes origin. Of course, rotation around the origin by an angle ϕ moves point (x,y) into (X,Y) via

$$\begin{bmatrix} Y \\ X \end{bmatrix} = \begin{bmatrix} \cos(\phi) & -\sin(\phi) \\ \sin(\phi) & \cos(\phi) \end{bmatrix} \begin{bmatrix} y \\ x \end{bmatrix}. \qquad (1)$$

Direct application of this formula leads to contours violating the three demands A, B, C, stated in B.1. In order to circumvent this, a "virtual" refinement of all pixels has been generated, creating a denser grid and rotation has been applied to it. Subsequently, to the resulting images, contours satisfying the demands above have been obtained by applying developed dedicated software.

B.3 Dividing the contour into blocks

Subsequently, the obtained contour is divided into blocks as follows:

A 3x3 pixels frame (mask) is shifted throughout the whole contour, so that, each time, a pixel of the contour is the centre of this mask. As usual, each square of the mask is labelled as shown in Figure 3a. This mask is used in order to enumerate the pixels of the contour as follows:

Each fragment contour frame is swept horizontally until the first contour pixel is encountered. This is the first pixel to become centre of the 3x3 frame. The pixel (1 or 2) of the 3x3 mask that is "occupied" (i.e. it belongs to the fragment contour), is unambiguously the next, #2 pixel, in the clockwise sense. Subsequently, the #2 pixel becomes the centre of the 3x3 mask. The pixel of the mask that is occupied by a contour pixel, other than pixel #1, becomes pixel #3 and so forth.

Next, using the pixel enumeration in the clockwise sense, the fragment contour is divided into blocks in the following way (see Figure 3): Pixels #1 and #2 belong to the first block. If pixel #3 is collinear with #1 and #2, i.e., if all three pixels are on the squares of the 3x3 mask labelled 6, C, 2, or 5, C, 1, and if #2, #3 and #4 pixels are collinear too, then pixel #3 belongs to block #1.

A block changes at the first pixel where the #(m-1) contour pixel, #m itself and the #(m+1) contour pixel are not collinear. Notice that the first pixel of each block might as well had belonged to the previous block (for example in Figure 4 pixel #4 might belong to block number 1 and 2, while pixel #9 might belong to block number 2 and 3). However, in this methodology it will be mainly considered that each such pixel will be the first pixel of the block with the greater cardinal number. Each time that a block changes, say at pixel #m, the relative angle is defined between the present and

the next block as the unique convex angle of the #(m+1) contour pixel in respect to #(m-1) contour pixel, according to the convention of absolute angles of all pixels of the 3x3 mask with the centre pixel C as shown in Figure 3b. Besides, it is useful for the applied method to define the absolute, so to say, angle of each block, which is the angle the block makes with the (x, y) axes of the fragment absolute frame of reference.

The block construction procedure ends when all contour pixels have been allocated to a block.

C. THE ACTUAL METHOD OF SPOTTING MATCHING FRAGMENTS

C.1 Defining the optimum matching parameters

One of the two fragments contours is arbitrarily considered as being fixed and by convention, the optimum matching figure to this contour is defined (see Figure 5). In fact, to each pixel of the fixed fragment its perfectly matching pixel corresponds as shown in Figure 5. It should be emphasized that the first pixel of each block has two matching pixels since for this application and only this, the first pixel of the block number m is considered to belong to the block number (m-1), too.

C.2 The notions of "fixed" and "rotating" chains

Suppose that two fragments are given and that one wants to decide if their contour shapes match and if yes, where they match. In order to achieve this, one first proceeds as follows:

One fragment is arbitrarily chosen to be fixed and it is placed in its absolute system of reference, which is called the "fixed fragment". Next, one considers a length of comparison measured in pixels, say COMP_LEN=250 pixels. At first, one considers a group of COMP_LEN consecutive pixels starting from pixel #1. This group of contour pixels is called "fixed chain".

Subsequently, the other to-be-compared fragment (called the "rotating" one) is considered at a specific orientation. A part of the contour of this rotating fragment is constructed around the fixed one as follows:

- The last pixel #M of the rotating fragment is placed in the **P**erfectly **M**atching **P**osition of pixel #1 of the fixed fragment, say in position PMP1.

- Next, a number of, say (k-1), subsequent pixels of the rotating fragment are placed in the absolute frame of reference of the fixed fragment, by parallel translation.
- The parallel translation of the rotating fragment, say B, in the absolute frame of reference of the fixed fragment, say A, ends when the last #k pixel of B contour, satisfies one of the following:

a) If one considers the direction along the average absolute angle of the last L pixels of the fixed chain and computes the line at right angles to this direction, which will be called "barrier" line, one stops the building of the "rotating chain" when it intersects the barrier line (see Figure 6). A consistent choice is to set L equal to COMP_LEN. However, the methodology manifests the same efficiency for smaller values of L, too, provided that L is greater than a lower bound LB_L. A good choice seems to be $LB_L = 0.45 * COMP\_LEN$.

b) If k is greater than a number of pixels called EXC_LEN and condition a) has not occurred; in this case one considers that, *de facto*, the two contours do not match for this position and orientation of fragments A and B. A good choice seems to be: EXC_LEN =2* COMP_LEN. We would like to stress that, although this demand may at a first glance seem as a matching criterion, however this is not the case. This demand is in fact set just to speed up the whole process. One may increase the value of EXC_LEN as much as one desires or cannot even use such a bound. We have simply made this choice just because extended experiments confirm that, when k becomes greater than 1.2* COMP_LEN then the considered fragments have always violated the matching criteria described below.

This procedure may be repeated for other considered orientations of the rotating chains too, as it will be described in Section D.

By repeating the same steps, and if M is the total number of contour pixels of the rotating fragment and N the total number of contour pixels of the fixed fragment, then rotating chains are sequentially built, starting every time from pixel $\#(M-j)$, $j = 1,2,...,M-1$, around the fixed chains, $\#\ell, \#\bmod_N(\ell+1),$ ...,$\#\bmod_N(\ell+\text{COMP\_LEN -1})$ $\ell = 2,3,...,N$ of the fixed fragment.

C.3 The first area matching criterion

Following a rather typical mathematical criterion, we consider that a measure of shape matching between the fixed chain of length COMP_LEN and the rotating chain of varying length, is the number of pixels enclosed by those two chains and the chain of pixels bridging the last pixels of the fixed and rotating chains (see Figure 6, 7). Notice, that at this stage one counts both the pixels that belong to the gap between the two fragments and those belonging to the two fragments. One does not count, however, neither the pixels of the fixed chain, nor the pixels of the rotating chain that are found to be at a Perfect Matching Position. Therefore, we consider that the contour of two fragments, say A and B, match at pixels $\#P_A$ and $\#P_B$ respectively, if the number of enclosed pixels between the corresponding chains defined above, is less than a chosen number, say MAX_AREA. The proper choice of MAX_AREA depends on the expected degree of decay the fragments have suffered, as well as the chosen COMP_LEN and the used resolution for the scanning of the fragments photos. In the extreme case, where no decay is expected, one may choose a very small value of MAX_AREA. With such a choice, one can apply the methodology developed here in order to solve the puzzle of perfectly matching pieces. In the archaeological problem we faced, however, an essentially greater number of MAX_AREA must be chosen to take into account the essential decay of the excavated fragments. It should be stressed that this MAX_AREA refers to the optimal case where the two adjacent fragments have the correct orientation in space. Since a random rotation of the two fragments in their absolute frame of reference exists, proper rotations of the rotating fragment must take place before a decision is taken, as it will be described in section D.1**.** Notice, that even for the correct orientation of the rotating fragment, as the value of MAX_AREA grows, there is a non-zero probability that accidental erroneous matching between two chains occurs (see Appendix B). This is due to the fact that if the previous, say m, pixels of the contour are given, then the #(m+1) contour pixel has a limited number of possible positions both for the fixed and the rotating chain. An estimation of the relation between MAX_AREA and COMP_LEN that has proven to be very efficient in practice, is given in Appendix B. Summarizing, one may state that for a given set of fragments and a given COMP_LEN it is possible to choose MAX_AREA values that essentially minimize random erroneous matching

occurrences. In order to further, drastically reduce the number of the erroneous matching occurrences between the fixed and rotating fragment, two other criteria have been used, based on contour information, that are subsequently defined.

C.4 The second area matching criterion

Suppose that the first matching criterion is satisfied for fragments A and B at pixels $\#P_A$ and $\#P_B$ respectively, for a specific rotating chain. If this were an actual matching position, no overlapping between the two adjacent fragments occurs, in the sense that all pixels enclosed by the fixed and the rotating chain should lay in the gap between the two fragments. Hence, the second matching criterion could be the demand that this condition actually occurs. However, in practice, small deviations from the fragments perfect depiction occur, due to imperfections in the shooting and image processing procedures. Then, as a second matching criterion, one demands that the number of pixels enclosed by the fixed and the rotating chain and lay in the gap between the two fragments, is a considerable percentage, say GP of the total number of enclosed pixels (see Figure 7). The extended experiments performed show that, for the given shooting and image processing procedures, a very good choice seems to be $GP = 0.997$. Clearly, the exact value of GP, as well as of MAX_AREA should be calibrated according to the needs and conditions of the application in hand. A presentation of the possible ill effects associated with a different choice of GP and other parameters values, is given in Appendix C.

C.5 The third area matching criterion

Suppose that the first and second matching criteria are satisfied for two fragments A and B at pixels $\#P_A$ and $\#P_B$ respectively, and for a certain relative orientation of A and B. At these specific positions and orientation one continues building the fixed and rotating chains until the entire contour of fragments A and B is formed (see Figure 7). As a third criterion one demands that the number of overlapping pixels between the interior of the two fragments contour is smaller than a lower bound, say LB, for the same reasons explained in C.4 above. A nice choice seems to be a dynamically

defined LB, as a percentage of the maximum contour of the two fragments, say LBP, since the greater the contour length of the two fragments, the greater the probability that their interiors overlap when A and B do not match. I.e., we let $LB = LBP * \max\{length(contour(A)), length(contour(B))\}$.

The extended experiments performed, show that, for the given shooting and image processing procedures, a very good choice seems to be $LBP = 0.996$.

C.6 The "sum of angles difference" matching criterion

We prove in Appendix A that, if one defines the "sum of angles" SA for any curve as

$$SA = \sum_{\substack{chain \\ pixels}} block\ angle \qquad (2)$$

then, if the maximum area enclosed by a fixed and rotating chain is E, there is a specific maximum, say $\mu_{\max}$, of the difference of the "sum of angles" of these two chains. To be precise, if d is the Euclidean distance between the beginning and end of the fixed chain and if, in order to write a more concise formula, we let $L = \text{EXC\_LEN}$, then,

$$\mu_{\max} = \sqrt{d^2 + \left(\frac{2*E}{d}\right)^2} \arctan\left(\frac{2*E}{d^2}\right) + \left(L - \sqrt{d^2 + \left(\frac{2*E}{d}\right)^2}\right)\frac{\pi}{2} \qquad (3)$$

Therefore, in order to decide if the previously mentioned area criteria will be applied for a couple of chains starting at pixels $\#P_A$ and $\#P_B$, the "sum of angles difference" matching criterion is applied first, stating that, if the sum of angles of the fixed and rotating chain differ more than $\mu_{\max}$, then, *de facto*, the two contours do not match for this position and orientation of fragments A and B. We would like to emphasize that the demand that the difference of the sum of angles of the fixed and rotating chain is small enough is not a sufficient condition for matching.

Notice that, since the orientation of the rotating fragment in its absolute frame of reference is completely random, in order to check matching between two fragments A and B, one must apply the three aforementioned area criteria for all chains starting at any couple of pixels $\#P_A$ and $\#P_B$ and for all possible relative orientations of the fixed and rotating fragment obtained with a certain quantized

rotation step $STEP$. To be more specific, one must rotate the rotating fragment B by $STEP$ degrees and, each time, must perform M*N area computations and comparisons. Thus, to exhaust all possible orientations of the rotating fragment one must perform $\frac{360}{STEP}$*M*N area computations and as many comparisons. In order to obtain accurate matching, $STEP$ must be small enough, e.g. $STEP \le 1^0$, resulting to tremendous time consumption. By applying the "sum of angles difference" criterion, we have succeeded in drastically reducing the total number of area computations and comparisons. In fact, in practice we have reduced the total time of comparison of two fragments by a factor of about twenty (20) or equivalently to five (5) percent of the overall time, by applying this fourth criterion.

D. APPLICATION OF THE AFOREMENTIONED METHODOLOGY

D.1 Implementation of the introduced methodology

A system has been developed implementing the aforementioned matching criteria as follows:

The total number of contour pixels is computed for all fragments (pieces). The application of the method starts with the fragment of greater number of contour pixels called "reference" fragment, tested for matching with all other fragments contour of the set, sequentially. In other words, the reference fragment is considered to be the fixed one, while all other are sequentially considered to be rotating fragments. For each couple of fixed and rotating fragments the following procedure, consisting of four steps at most, is applied.

Step 1: For a specific rotating fragment, the procedure described in C.2 is initially applied for the orientation of the contour of this fragment in its absolute frame of reference (see B.2). For this orientation, the system, starting every time from pixel $\#(M_k - j), j = 0,1,2,...,M_k - 1$, of the rotating fragment, sequentially builds rotating chains around the fixed chain consisting of pixels $\#\ell$, $...,\#\mathrm{mod}_N(\ell + \mathrm{COMP\_LEN} - 1)$ $\ell = 2,...,N$, where M_k is the number of contour pixels of the rotating fragment $\#k$ while N the number of contour pixels of the reference fragment (see Figures 5, 6).

Step 2: For the orientation of the contour of the rotating fragment in its absolute frame of reference, and for every couple of chains starting at ℓ, j respectively, the aforementioned "sum of

angles difference" criterion is applied (see C.6). Namely, the "sum of angles" of both the fixed and rotating chain is computed, say SA_f and SA_r, and if $abs(SA_f - SA_r) > \mu_{\max}$, then we consider, *de facto*, that the two contours do not match at this position for this orientation. On the contrary, if $abs(SA_f - SA_r) \le \mu_{\max}$ holds, then we proceed to Step 3 described below.

Step 3: The number of enclosed pixels $E_{\ell,j}$ between the fixed and rotating chains as well as the number $G_{\ell,j}$ of pixels lying in the gap between these two fragments are computed. If $E_{\ell,j}$ is smaller than a specific threshold T and $G_{\ell,j}$ satisfies the second matching criterion, then the system considers that the two fragments in hand may match at the couple of pixels (ℓ, j). The value of the threshold T may be computed as follows: Suppose that (ℓ, j) is an actual matching position of the two fragments in hand. Then, $T = MAX\_AREA + Q_R$, where MAX_AREA is chosen to take into account fragments decay as described in section C.3, while Q_R is an error due to the quantization of rotation. A good estimate for the maximum value of Q_R is

$$\max(Q_R) = \frac{1}{2} COMP\_LEN^2 \tan\left(\frac{STEP}{2}\right) \qquad (4)$$

where $STEP$ is the quantization step of rotation. We have chosen $STEP = 1^0$, therefore $T_1 = MAX\_AREA + 0.0044 COMP\_LEN^2$. Thus, if for a couple of pixels (ℓ, j), it holds

$$E_{\ell,j} \le T_1 \qquad (5)$$

and if $G_{\ell,j}$ satisfies the second matching criterion (C.4), then one proceeds to checking if the third matching criterion holds. If this criterion is satisfied, too, the system decides conclusively that the two fragments in hand may match at these two pixels. Otherwise, if one of the aforementioned area criteria is not satisfied, the system decides that no matching is possible between the reference fragment and the specific orientation of the rotating fragment at (ℓ, j). In other words, if there is an actual matching between the two fragments at a couple of pixels (ℓ, j), due to their contour shape characteristics alone, then this couple must belong to the set suggested by the system.

Step 4: Finally, all three steps above are repeated for all possible orientations of the rotating fragment obtained via successive rotations of this fragment with rotation step $STEP = 1^0$.

Each fragment the system suggests that it might match with the reference fragment, and the reference fragment itself, are concatenated at the exact positions (ℓ, j), by means of a proper C code. The obtained greater fragment consisting of the concatenated matching ones is used as input to an image-processing tool. In this way the user is able to visualise the system proposition and is able to decide whether this is correct or not. Next, the actually matching fragments are concatenated to form a new single "artificial" fragment and the whole aforementioned procedure is repeated. The fixed reference fragment is considered now to be the big "artificial" piece constructed above. This procedure is repeated until no further matching occurs. In this way, an “island” of matching fragments is formed. Should fragments of the set in hand remain, the whole aforementioned procedure is repeated with reference fragment the one of greater contour length not belonging to the previously constructed island(s), until all fragments are exhausted. Notice, that a histogram of the contour lengths of all initial fragments is formed, and if a considerable variance in the contour lengths is observed, then the whole aforementioned procedure is repeated and for other comparison lengths $COMP\_LEN$, too.

D.2 Experimental results

In order to test the introduced methodology as well as the developed system we have separately applied it to two different chosen sets of fragments. The first set comprised two hundred sixty two (262) fragments belonging to two different wall-paintings that have already been reconstructed by technicians and archaeologists, who devoted a considerable number of man-months. On the contrary, the second set comprised nine hundred thirty six (936) fragments belonging to several wall-paintings that have not been reconstructed yet. It must be pointed out that, although the specialised personnel has made a serious effort toward this direction, no considerable matching between fragments of this second set has been found due to the large number of pieces, their size, the

thematic content of the wall-paintings that made many fragments look alike and the fact that a serious number of fragments was missing.

Concerning the first set of fragments forming the already constructed wall-paintings we have used the following parameter values: a) Two different values of COMP_LEN: First 170, then 110, b) EXC_LEN =2* COMP_LEN, c) MAX_AREA=350 pixels and 250 respectively

A brief description of the most significant parameters physical content, a reasoning for the adopted values of them, as well as a presentation of the possible ill effects associated with a different choice of each parameter value, are given in Appendix C.

The system started considering No 46 to be the first "reference" fragment. The system suggested that the only possible matches for fragment No 46 are the ones shown in Table 1. In addition to the possible matching fragments, the system obviously offered the exact orientation of the absolute frame of reference of the rotating fragment as well as the exact matching position (ℓ, j). All suggestions of the system concerning No 46 were absolutely correct and they were adopted.

Subsequently, we let all the matching to No 46 fragments together with No 46 itself form a new single "artificial" fragment ("island" of fragments) and we repeated the same procedure with this "island" being the new reference fragment and so on, until no further matching occurred. In order to speed up the process, we didn't re-examine fixed chains that belonged entirely to previously checked fragments. Notice that, frequently, the first matching criterion was correctly satisfied for two or few more neighbouring contour pixels of the fixed chain. At this point, a considerable bulk of the first wall-painting has been completed successfully (see Figure 8). Notice that for readability reasons, the initial enumeration has been changed in the wall-painting figure.

Then, we picked the non-matching fragment with greater number of contour pixels and we repeated the aforementioned procedure in order to form a separate block of fragments, with COMP_LEN=170 pixels once more. After few iterations, the user was able visualise that in this way, a second wall-painting started being reconstructed. When no further matching was reported by the system, a main bulk of the second wall painting was formed, too. This procedure was repeated for the remaining fragments with a smaller COMP_LEN =110 pixels. This time, the system reported

correctly the proper matching positions, but at the same time proposed other matching possibilities, that have been rejected by the user due to the colour or subject non-continuity.

Notice, that similar table to 1 presented here, exist for the second reconstructed wall-painting too, but it has not been included for space economy reasons. We must point out that the relatively small values of the area between fixed and rotating chains at the matching positions, indicate that the wall-painting in hand has suffered no serious decay and damage.

The most serious test of the introduced methodology and the related system was its application to a set of fragments belonging to wall-paintings that have not been previously reconstructed. In fact, nine hundred thirty six (936) fragments belonging to several wall-paintings, have been, for the first time, photographed by the authors under strict photographic conditions. The area of the fragments varied from approximately $1cm^2$ to approximately $3000cm^2$, the more frequently encountered one being about $100cm^2$.

After the initial processing to improve the quality of the obtained images and isolate the fragments as described in B.1, the main reconstruction procedure has been applied.

Concerning this second set of fragments we have used the following parameter values:

a) Two different values of COMP_LEN: First 300, subsequently 250, b) EXC_LEN =2* COMP_LEN c) MAX_AREA=1400 pixels and 1200 respectively

In connection with the above parameter values choice we must point out the following:

We have chosen relatively large values of MAX_AREA to account for expected considerable decay and damage of fragments. We have chosen relatively large values of COMP_LEN for two reasons: First, because the average perimeter length of the fragments was high enough and second due to the large number of fragments in this second set (see Appendix B).

Starting with the greater contour fragment, we repeated the aforementioned procedures forming islands of matching concatenated fragments. We show two of these islands, not previously reconstructed by scholars, in Figures 9 and 10.

We emphasize that we have tried to be very careful in choosing the value of MAX_AREA, to reduce the number of accidental erroneous matching between two fragments (see C.3 and Appendix

B). In this way, in about 60% of the fragments reported to match, no erroneous matching took place due to accidental contour shape resemblance. In the rest 40% of fragments one to five (1-5) accidental matchings per fragment have been reported. Reducing the MAX_AREA would practically almost exponentially reduce the number of occurrences of accidental contour shape matching, but in this case we would not be able to account for the relatively big gaps existing between adjacent fragments caused by serious decay and/or by the violence of the breaking procedure. The rejection of the erroneous accidental matching has been made by inspection of the fragments. To obtain an as much as possible automated reconstruction of images from its constituent fragments, one must take into consideration other parameters, too, such as: 1) Colour continuation between actually adjacent fragments, 2) Depicted objects contour continuation, 3) Thematic content continuation, 4) Width of the fragment vertically to its depiction surface, 5) Geological texture of the side opposite to the painted one, etc. The aforementioned are the object of extended study by our team and the related results will be published shortly.

Finally, the hardware infrastructure was Pentium III 550 MHz, 256 MB RAM and SCSI HDDs of total capacity 20 GB approximately. The operational system was Red Hat Linux in dual boot with Windows 95.

CONCLUSION

In this paper a new methodology is introduced for the computer-aided reconstruction of the Thera (Santorini) wall-paintings, painted in the middle of the second millennium BC. These wall-paintings are excavated in fragments and in order to facilitate and speed up their reconstruction process, a system has been developed based on the proposed methodology. Both the system and the methodology presented here, extract the maximum possible information from fragments contour shape to point out possible fragments matching. The methodology and the system have been used to reconstruct two excavated wall-paintings consisting of 262 fragments, with full success, but most important have been used to reconstruct, for the first time, unpublished wall-paintings parts from a set of 936 fragments.

APPENDIX A

Consider all simple curves starting from a specific point A and ending to a certain point Γ belonging to the straight line vertical to AB, as in Figure 11. Consider, in addition, the subset S_E of all these curves with length smaller than a certain upper bound, say EXC_LEN, which, together with the straight line segments AB and BΓ form a closed simple curve of constant area, say E.

Consider any such curve $C \in S_E$ with parametric representation say $x(t), y(t)$. If at an arbitrary point M of C one computes the angle of the tangent of C at M with the x-axis, say θ, (Figure 11), then we need to find the curve that generates the maximum possible sum of these angles and the value of this sum. In other words, in a sense, we want to spot the curve belonging to the class S_E that has the greater integral of slopes. We state the problem in mathematical terms as follows:

We seek extremization of the integral $\mu_f = \int_A^\Gamma \arctan\left(\frac{\dot{y}_f(t)}{\dot{x}_f(t)}\right) dt$ (A.1)

under the restriction $E_C = \int_A^\Gamma (x\dot{y} - y\dot{x})dt = \text{E} = \text{Constant}$ (A.2)

Going along lines of Calculus of Variations, in order to achieve this, we extremize the integral $I = \int_C f(t, x, \dot{x}, y, \dot{y})$, where $f(t, x, \dot{x}, y, \dot{y}) = \arctan\left(\frac{\dot{y}_f(t)}{\dot{x}_f(t)}\right) + \lambda(x\dot{y} - y\dot{x})$ and λ a Lagrange multiplier. Then this extremization demand leads to the Euler- Lagrange equations

$$\frac{\partial f}{\partial x} - \frac{d}{dt}\left\{\frac{\partial f}{\partial \dot{x}}\right\} = 0 \qquad \text{(A.3)} \qquad\qquad \frac{\partial f}{\partial y} - \frac{d}{dt}\left\{\frac{\partial f}{\partial \dot{y}}\right\} = 0 \qquad \text{(A.4)}$$

together with the boundary conditions $f(A) = 0$ (A.5), $\frac{\partial f}{\partial \dot{x}}(\Gamma) = 0$ (A.6)

Rather straightforward calculations lead to the system of linear equations

$$y + \frac{\dot{y}}{\dot{x}^2 + \dot{y}^2} = C_1 \qquad \text{(A.7)} \qquad\qquad x + \frac{\dot{x}}{\dot{x}^2 + \dot{y}^2} = C_2 \qquad \text{(A.8)}$$

Combining (A.7), (A.8) together with (A.5) and (A.6) and after some calculus, we obtain that

the solution is a piece-wise straight-line leaving A and ending in line (ε) as shown in Figure 12, where the curve length L has been taken into consideration, too. Since, an upper bound $\mu_{\max}$ for μ_r clearly exists, then this is the sought for maximal "integral of angles" curve as it is confirmed by geometric inspection, too.

The angles integral $\mu_{\max}$ for this curve is.

$$\mu_{\max} = \sqrt{d^2 + \left(\frac{2*E}{d}\right)^2} \arctan\left(\frac{2*E}{d^2}\right) + \left(L - \sqrt{d^2 + \left(\frac{2*E}{d}\right)^2}\right)\frac{\pi}{2} \qquad \text{(A.9)}$$

Since, we always choose the x-axis to be the straight line connecting the beginning and end of the fixed chain and since $\mu_{\max}$ is an increasing function of E, it follows that this is the sought for dynamically calculated maximum of the difference of "sum of angles" between the fixed and rotating chain.

To set ideas, the most frequent in practice values of the length L of the rotating chain and of d, lie in the following intervals:

$L \in [1.01, 1.06]*COMP\_LEN$, $d \in [0.95, 0.99]*COMP\_LEN$.

Then, for $COMP\_LEN = 250$, L =1.03*$COMP\_LEN$, d=0.97 *$COMP\_LEN$ and E= 1300, the value of the "sum of angles" maximum difference between the fixed and rotating chains, is $\mu_{\max} = 1943.2$, corresponding to an average angle of approximately 7.5° or, equivalently, to an angle $\Gamma\hat{A}B = 6^\circ$ of the straight lines joining the beginning and the end of the two chains.

APPENDIX B

Suppose that two fragments contours are compared in order to spot possible matching between them. An accidental erroneous matching occurs when the system suggests a couple of pixels for possible contour matching that does not actually exist due to other criteria violation such as colour and depiction continuation. In order to obtain a valid estimation of MAX_AREA that drastically reduces the number of accidental erroneous matchings in practice, we have applied the following statistical method:

We have developed a "random generator" of chains of pixels of a chosen length subject to the restrictions stated in B.1. In other words, starting from two adjacent initial pixels we have constructed two chains by consecutively adding new pixels where each new pixel was chosen randomly with equal probability among all its possible positions permitted by the restrictions stated in B.1. The first of the two chains is of length COMP_LEN, while the other one ends as described in C.2. For every couple of chains we have computed the number NEP of pixels they enclosed as well as the number NXP of pixels found in the "external" of the two chains considering that the one chain is constructed clockwise while the other is constructed counter-clockwise, as described in C.2 and D. By repeating this procedure many times for many different couples of chains we have obtained a significant statistical sample showing the number and relative percentage RP of NEP occurrences for various COMP_LEN. A part of the plot of the relative percentage RP of each NEP appearance for COMP_LEN=250 pixels and for 10^{11} random couples of chains is shown in Figure 13. Notice, that the percentage of appearance of couples of chains where the one exceeded EXC_LEN or couples of chains with $NEP \geq 5000$ is 99% and it is not depicted in Figure 13. In addition we have obtained the number and the percentage of "external" pixels in each case. A part of the plot showing these results for COMP_LEN=250 pixels is shown in Figure 14. From these figures it is obvious that for a COMP_LEN=250 pixels, a choice of MAX_AREA<=1100 pixels drastically reduces the number of accidental erroneous matchings or it even eliminates them. Therefore, as expected, proper choice of MAX_AREA is a compromise between user's desire to incorporate fragments decay and reduction of the number of accidental erroneous matchings.

APPENDIX C

Description of the introduced parameters and implications of their value choice

COMP_LEN: The number of pixels of every fixed chain.

The parameter value is clearly associated with the expected minimum contact length between two adjacent fragments. The smaller its value, the greater the probability of

spotting all actual matches in a set of fragments and vice versa. But, at the same time, the greater the number of accidental erroneous matchings.

EXC_LEN: The maximum number of pixels of every rotating chain.

A parameter chosen to speed up the whole process, since actual contact curves between matching fragments cannot differ dramatically in length.

GP : The lower limit of the percentage of pixels enclosed by each couple of fixed and rotating chain and lay in the gap between two compared fragments.

Setting the value of this parameter equal to one (1) is inappropriate since, in this case, one cannot account for small deviations from the fragments perfect depiction occurring, due to imperfections in the shooting and image processing procedures. The smaller the value of GP , the smaller the probability of missing an actual match, but, at the same time, the greater the number of false matches.

LB : The upper limit of overlapping pixels between the interior of the two fragments for each comparison (Same comment as above).

MAX_AREA: The upper limit of pixels number enclosed by each couple of fixed and rotating chain for which the system signals possible matching.

The proper choice of MAX_AREA depends on the expected degree of decay the fragments have suffered, as well as the chosen COMP_LEN and the used resolution of the fragments digitized photos. The greater its value, the greater the probability of spotting all actual matches in a set of fragments and vice versa; but, at the same time, the greater the number of accidental erroneous matchings.

BIBLIOGRAPHY

[1] Christos Doumas, “The Wall-Paintings of Thera”, The Thera Foundation Petros Nomikos, Athens, 1999, Kapon Editions.

[2] R. T. Chin and C. R. Dyer, “Model-based recognition in robot vision”, ACM Computing, 18(1):67-108, March 1986.

[3] P. Pudil, J. Novovicova and J. Kittler "Simultaneous Learning of Decision Rules and Important Attributes for Classification Problems in Image Analysis", Image and Vision Computing, 12:193-198, 1994.

[4] P. J. Besl and R. C. Jain, "Three-dimensional object recognition", Computing Surveys, 17(1):75-145, March 1985.

[5] D. G. Lowe, "Three-dimensional object recognition from single two-dimensional images", Artificial Intelligence, 31(3):355-395, 1987.

[6] R. A. Brooks, "Model-based three-dimensional interpretations of two-dimensional images", IEEE Trans. Pattern Analysis and Machine Intelligence, 5(2):140-149, 1983.

[7] R. A. Brooks, R. Greiner, and T. O. Binford, "The acronym model-based vision system", In Int. Joint. Conf. Artificial Intelligence, 1979.

[8] J. F. Canny, "A computational approach to edge detection", IEEE Trans. Pattern Analysis and Machine Intelligence, 8(6):679-698, November 1986.

[9] T. F. Knoll and R. C. Jain, "Recognizing partially visible objects using feature indexed hypotheses", IEEE J. Robotics and Automation, 2(1):3-13, March 1986.

[10] G. J. Ettinger, "Large hierarchical object recognition in robot vision", Proc. Conf. Computer Vision and Pattern Recognition, pages 32-41, 1988.

[11] W. E. L. Grimson, "Recognition of object families using parameterized models", Proc. First International Conf. Computer Vision, pages 93-101, 1987.

[12] Y. Lamdan, J. T. Schwartz, and H. J. Wolfson, "Object recognition by affine invariant matching", Proc. Conf. Computer Vision and Pattern Recognition, pages 335-344, 1988.

[13] C. Hansen and T.C. Henderson, "CAGD-based computer vision", IEEE Trans. Pattern Analysis and Machine Intelligence, 11:1181-1193, November 1989.

[14] B. Bhanu and C. Ho, "CAD-based 3-d object recognition for robot vision", Computer, 20(8):19-36, 1987.

[15] L. G. Shapiro, "A CAD-model-based system for object localization", Proc. SPIE Digital and Optical Shape Representation and Pattern Recognition, 938:408-418, 1988.

[16] N. Narasimhamurti and R. C. Jain, “Computer-aided, design-based object recognition: Incorporating metric and topological information”, Proc. SPIE Digital and Optical Shape Representation and Pattern Recognition, 938:436-443, 1988.

[17] J. J. Koenderink and A. J. van Doorn, “The singularities of the visual mapping”, Biological Cybernetics, 24:51-59, 1976.

[18] J. J. Koenderink and A. J. van Doorn, “The internal representation of solid shape with respect to vision”, Biological Cybernetics, 32:211-216, 1979.

[19] I. Chakravarty and H. Freeman, “Characteristic views as a basis for three-dimensional object recognition”, Proc. SPIE Conf. Robot Vision, 336:37-45, 1982.

[20] Z. Gigus and J. Malik, “Computing the aspect graph for line drawings of polyhedral objects”, IEEE Trans. Pattern Analysis and Machine Intelligence, 12(2):113-122, 1990.

[21] D. Eggert and K. Bowyer, “Computing the orthographic projection aspect graph of solids of revolution”, Proc. IEEE Workshop on Interpretation of 3-D Scenes, pages 102-108, 1989.

[22] D. J. Kriegman and J. Ponce, “Computing exact aspect graphs of curved objects: Solids of revolution”, Proc IEEE Workshop on Interpretation of 3-D Scenes, pages 116-122, 1989.

[23] T. Sripradisvarakul and R. C. Jain, “Generating aspect graphs for curved objects”, Proc. IEEE Workshop on Interpretation of 3-D Scenes, pages 109-115, 1989.

[24] P. Arabie, L. J. Hubert and G. De Soete, editors.”Clustering and Classification”, World Scientific, River Edge, NJ, 1996.

[25] R. Nevatia, “Machine Perception”, Prentice-Hall, New Jersey 1982.

[26] D. Marr and E. C. Hildreth, “Theory of edge detection”, Proc. R. Soc. Lond. B, 207:187-217, 1980.

[27] R. Jain, R. Kasturi and B. Schunck, “Machine Vision”, McGraw-Hill, 1995.

[28] K. Hirota and Y. Ohto, "Image Recognition in Jigsaw Puzzle Assembly Robot Systems", Bull. Coll. Eng., Hosei Univ., Japan, pp. 87-93, May. 1986.

[29] G. C. Burdea and H. J. Wolfson, "Solving Jigsaw Puzzles by a Robot", IEEE Transactions on robotics and automation, Vol. 5, No. 6, December 1989.

[30] D. A. Kosiba, P. M. Devaux, S. Balasubramanian, T. L. Gandhi and R. Kasturi, "An Automatic Jigsaw Puzzle Solver", IEEE Conference 1994.

[31] R. W. Webster, P. S. LaFollette and R. L. Stafford, "Isthmus Critical Points for Solving Jigsaw Puzzles in Computer Vision", IEEE Trans. on Systems, Man and Cybernetics, Vol. 21, No. 5, September/October 1991.

[32] R. W. Webster and P. W. Ross, "A Computer Vision System that Assembles Canonical Jigsaw Puzzles using the Euclidean Skeleton and Isthmus Critical Points", IAPR Workshop on Machine Vision Applications, Nov. 28-30, 1990, Tokyo.

[33] G. Radack, N. Badler, "Jigsaw Puzzle Matching using a Boundary Centered Polar Encoding", Computer Graphics and Image Processing, Vol. 19, pp. 1-2, May 1982

[34] H. Freeman and L. Garder, "A Pictorial Jigsaw Puzzle: The Computer Solution to a Problem in Pattern Recognition", IEEE Trans. Electron. Comput., Vol. EC-13, pp. 118-127, Apr. 1964.

[35] K. Nagura, K. Sato, H. Mackawa, T. Morita and K. Fujii, “Partial Contour Processing using Curvature Function – Assembly of Jigsaw Puzzle and Recognition of Moving Figures”, Syst. Computing, Vol. 2, pp. 30-39, Feb. 1986.

[36] P.J. Olver, G. Sapiro and A. Tannenbaum, “Invariant geometric evolutions of surfaces and volumetric smoothing”, SIAM, J. Appl. Math. 57, pp. 176-194, 1997.

[37] P.J. Olver, “Joint invariant signatures”, Found. Comput. Math. 1, 3-67, 2001.

[38] A. Zisserman, D. Forsyth, J. L. Mundy, C. Rothwell, J. Liu and N. Pillow, “3D Object Recognition Using Invariance”, Elsevier, Artificial Intelligence 78(1-2), pp. 239-288, 1995.

[39] P.J. Olver, G. Sapiro, and A. Tannenbaum, “Affine invariant detection: edge maps, anisotropic diffusion, and active contours”, Acta Appl. Math. 59, pp. 45-77, 1999.

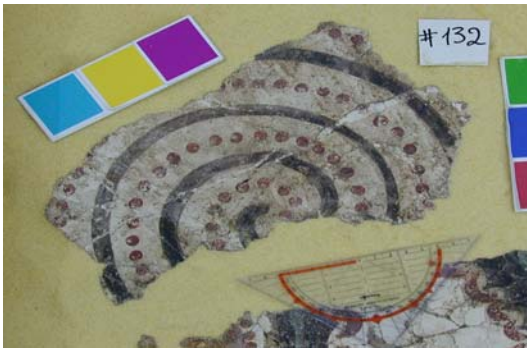

Figure 1

The actual embedded fragments image

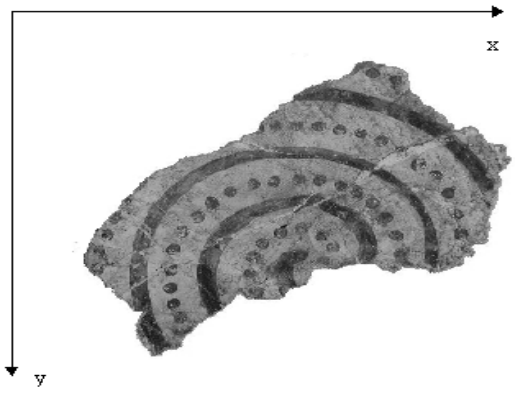

Figure 2

A fragment in its "absolute reference system" with the (x, y) axes

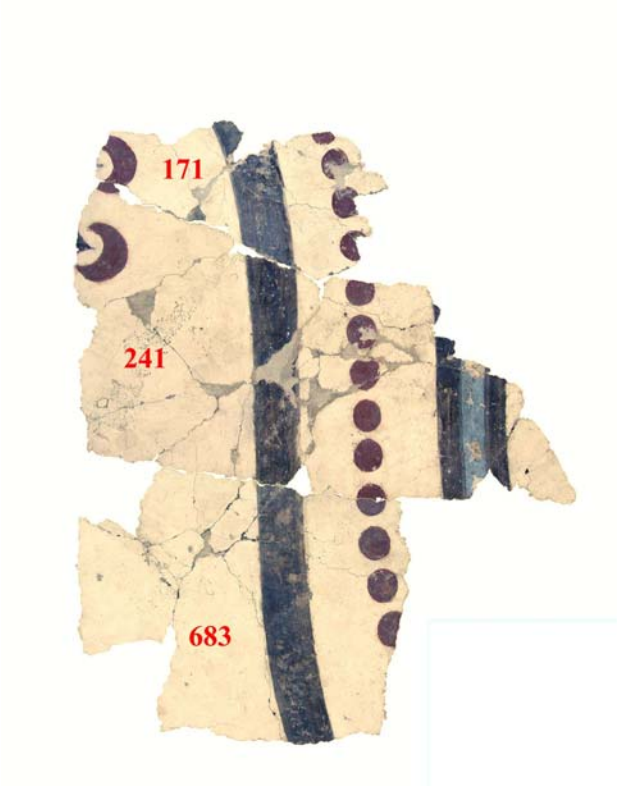

Figure 9

First island of fragments

Figure 10

Second island of fragments

6	7	8
5	C	1
4	3	2

Figure 3a

Indexing the pixels of the 3x3 mask.
C is the center pixel of the mask that belongs to the contour

135	90	45
180	C	0
-135	-90	-45

Figure 3b

Depiction of absolute angles of all pixels of the 3x3 mask with the center pixel C

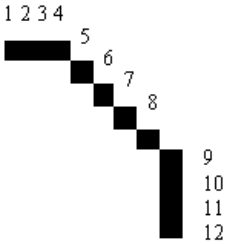

Figure 4

Block Number 1: Pixels #1, #2, #3.
Block Number 2: Pixels #4, #5, #6. #7, #8.
Block Number 3: Pixels #9, #10, #11.
Pixel #12 is the beginning of **Block Number 4.**

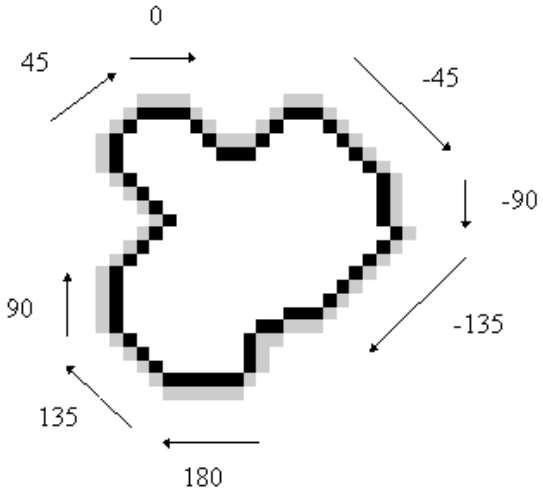

Figure 5

Depiction of the optimum matching figure to a fragment contour. With black colour the fragment contour. With grey colour its optimum matching figure.

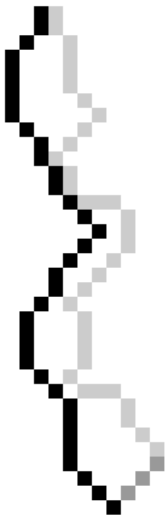

Figure 6

Depiction of "fixed" and "rotating" chain belonging to two different frescos (pieces).
Black pixels belong to the "fixed" chain.
Light grey pixels belong to the "rotating" chain.
Darker grey pixels bridge the last pixel of the two chains ("barrier" line).
Notice that the "rotating" (red) chain ends when it intersects the "barrier" line.

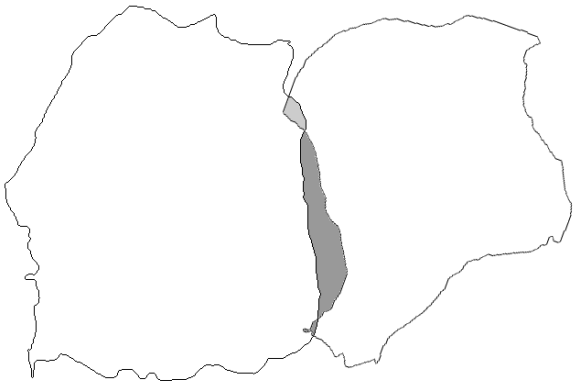

Figure 7

Entire contours of fragments A and B.
Light grey: pixels that belong to the two fragments
Darker grey: pixels that belong to the gap between the two fragments

Figure 8

Second island of fragments

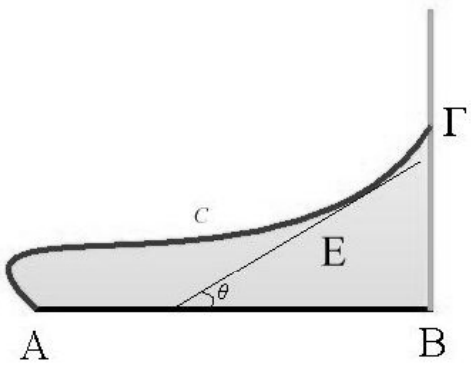

Figure 11

A curve starting from a specific point A and ending to a certain straight point Γ belonging to the line vertical to AB

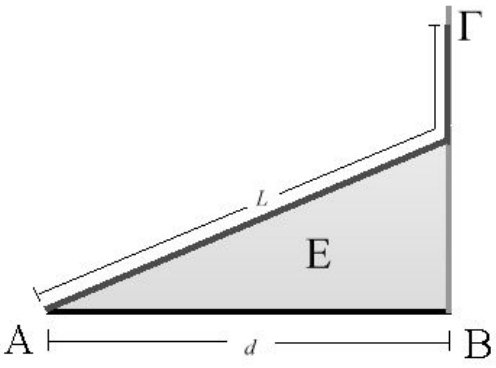

Figure 12

A piece-wise straight-line leaving A and ending in line (ε)

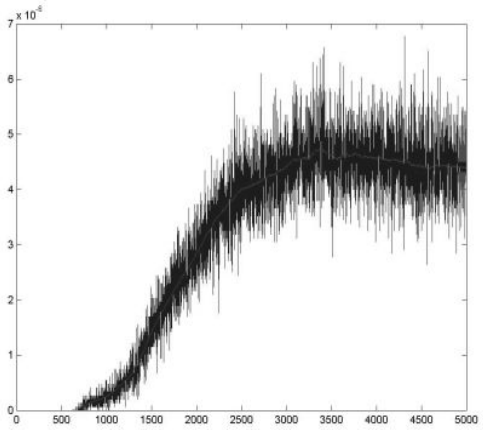

Figure 13

A part of the plot of the relative percentage RP of each NEP appearance for COMP LEN=250 pixels

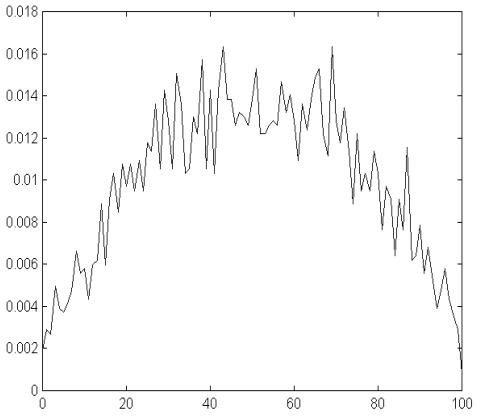

Figure 14

A part of the plot of the percentage of "external" pixels for COMP_LEN=250 pixels

COMP_LEN=170 PIXELS				
STEP	**FRAGMENT WITH WHICH COMPARISONS ARE MADE**	**MATCHING FRAGMENTS**	**MINIMUM AREA BETWEEN MATCHING FRAGMENTS**	**ERRONEOUS MATCHINGS**
1	46	34-47-48-111	160-253-127-103	NONE
2	FIRST ISLAND CONSISTING OF No 46,34,47,48,111	26-35-36-66-112	177-170-227-140-157	NONE
3	SECOND ISLAND CONSISTING OF FIRST PLUS 26, 35, 36, 66, 112	20-25-27-28-51-65	137-230-100-127-193-143	NONE
4	THIRD ISLAND CONSISTING OF SECOND PLUS 20, 25, 27, 28, 51, 65	14-15-21-37-50-64-67	110-203-47-200-63-197-223	NONE
5	FOURTH ISLAND CONSISTING OF THIRD PLUS 14, 15, 21, 37, 50, 64, 67	1-3-5-6-13-16-22-49-53-68-113	223-173-53-103-110-127-123-223-143-133-73	NONE
6	SIXTH ISLAND CONSISTING OF FIFTH PLUS 1, 3, 5, 6, 13, 16, 22,49,53,68,113	2-4-7-8-17-29-52-54-75-94	140-233-197-200-250-207-120-173-170-97	NONE
7	SEVENTH ISLAND CONSISTING OF SIXTH PLUS 2, 4, 7, 8, 17, 29, 52, 54, 75, 94	9-11-23-55-58-76-80-85-93	210-243-240-160-230-177-193-120-137	NONE
8	EIGHTH ISLAND CONSISTING OF SEVENTH PLUS 9,11,23,55,58,76,80,85,93	10-12-24-36-60-77-79-86-92	177-163-233-207-107-123-147-203-237	NONE
9	NINTH ISLAND CONSISTING OF EIGHTH PLUS 10,12,24,56,60,77,79,86,92	31-32-38-39-40-57-69-74-78-81-88-91	250-243-210-187-140-157-137-177-207-113-183-193	NONE
10	TENTH ISLAND CONSISTING OF NINTH PLUS 31,32,38,39,40,57,69,74,78,81,88,91	30-33-41-70-71-82	190-153-90-170-107-163	NONE
11	11-TH ISLAND CONSISTING OF 10-TH PLUS 30,33,41,70,71,82	42-45-72-83	177-147-137-120	NONE
12	12-TH ISLAND CONSISTING OF 11-TH PLUS 42,45,72,83	43-44-73-84-87-107	217-180-163-123-107-93	NONE
13	13-TH ISLAND CONSISTING OF 12-TH PLUS 43,44,73,84,87,107	95-106	63-190	NONE
14	14-TH ISLAND CONSISTING OF 13-TH PLUS 95,106	105-108	77-223	NONE
15	15-TH ISLAND CONSISTING OF 14-TH PLUS 105,108	109	243	NONE
16	16-TH ISLAND CONSISTING OF 15-TH PLUS 109	97-110	227-183	NONE
17	17-TH ISLAND CONSISTING OF 16-TH PLUS 97,110	96-104	123-233	NONE

Table 1
Observed values in the reconstruction of the Wall-painting presented in Figure 8